Osmotic Pressure of Dilute and Semidilute Polymer Solutions: A Comparison between a New Calculation and Old Experiments

Lothar Schäfer

Institut für Theoretische Physik der Universität, D-3000 Hannover, West Germany.
Received September 2, 1981

ABSTRACT: In a good solvent the osmotic pressure of polymer solutions shows universal scaling behavior as a function of chain length and concentration. We compare our recent calculation of this scaling function to an extensive set of measurements taken from the literature. The comparison includes both the dilute and the semidilute regime and shows that experiment and theory agree up to weight fractions of polymer of the order of 0.15. It is found that most experiments cover an intermediate concentration range where the chains overlap considerably. It therefore is not possible to extract values of the chain length or the virial coefficients without use of theoretical information. For shorter chains our theory is consistent with the use of a square root plot in the analysis of the data; for very long chains this method is likely to underestimate the chain length. Our calculation of the polydispersity dependence of the osmotic pressure contradicts previous theories, and we point out that previous theoretical work in some cases does not allow for a consistent interpretation of the data. Within the framework of our theory a consistent interpretation seems to be possible, but the experiments are not accurate enough to allow for definite conclusions.

1. Introduction

Since the work of Flory it is known that dilute solutions of long polymer molecules can be described within the framework of "two-parameter" theories. These theories assume that macroscopic properties of the solutions depend only on two parameters, one representing the interaction among any two segments of the chains, the other specifying the size of a noninteracting chain. During recent years these ideas have found a rigorous and most beautiful formulation in terms of the concepts of "scaling" and "universality". These concepts are taken from the theory of phase transitions, and the basic work of de Gennes[1] and des Cloizeaux[2] has established the connection between the phase transition problem and the description of polymer solutions. For instance, des Cloizeaux has proven a "scaling law" for the osmotic pressure Π as function of the concentration c_p of polymer chains and of the average number N of monomers per chain.

$$\frac{\Pi(c_p,N)}{RT} = c_p[1 + \mathcal{P}(bc_pN^{3\nu})] \tag{1.1}$$

This scaling law states that Π/RT, up to a trivial factor c_p, depends on the single combination $c_pN^{3\nu}$ of its variable c_p and N. This "scaling variable" is known as the "overlap".

$$s = bc_pN^{3\nu} \tag{1.2}$$

Universality of eq 1.1 means that only the scale b of s depends on the chemical constitution and the temperature of the solution. Both the exponent ν and the form of the function $\mathcal{P}$ are "universal", i.e., independent of such "irrelevant" variables.

The scaling law (1.1) holds in the excluded volume limit, i.e., for dilute or semidilute solutions of long chains in a good solvent, and in the derivation des Cloizeaux assumed a broad chain length distribution which is in equilibrium with respect to a hypothetical reversible polymerization reaction. The theory was soon extended[3] to moderately good solvents and Θ solvents. This introduces the second scaling variable $z = \beta N^{1/2}$, where β in essence gives the distance in temperature from the Θ point, $\beta \sim 1 - T/\Theta$. The approach thus extended covers the full domain of two-parameter theory. The excluded volume limit is found as z tends to infinity. Quite recently, we have been able to extend the theory to solutions of arbitrary polydispersity.[4] It is found that the scaling functions in the excluded volume limit depend not only on the scaling variable s but also on the reduced chain length distribution $p(y)$, which is related to the normalized probability $P(n)$ of finding a chain of n monomers.

$$P(n) = \frac{1}{N}p\left(\frac{n}{N}\right) \tag{1.3}$$

$$N = \sum_n nP(n) \tag{1.4}$$

Thus in the excluded volume limit $z \to \infty$ the generalized form of the law (1.1) reads

$$\frac{\Pi(c_p,P(n))}{RTc_p} = 1 + \mathcal{P}(s,p(y)) \tag{1.5}$$

where $\mathcal{P}$ is a universal functional of s and $p(y)$.

The new approach underlying scaling and universality is known as the renormalization group. It is by no means restricted to thermodynamic quantities, and it has been used to prove universal scaling laws for all correlation functions[5] one reasonably might hope to measure in a scattering experiment. The scaling laws, together with general thermodynamic relations, have also been used to show[4] that the functional $\mathcal{P}$ (eq 1.5) is the central thermodynamic quantity which determines the universal contributions to the average chemical potential, the excess enthalpy, and so on.

All the results mentioned up to now could be called "strong" results since they are the almost inevitable consequence of the structure of the theory. To be sure, they are strictly valid only in the limit $N \to \infty$, $Nc_p \to 0$, but in that limit their derivation does not involve approximations. The renormalization group theory also suggests that exponents like ν or scaling functionals like $\mathcal{P}$ can be calculated numerically by methods very similar to the well-known cluster expansions.[6] These calculations yield only "weak" results since they imply the termination of the expansions after the first few terms. It is only for the exponents that a detailed insight into the higher order behavior of the expansions has led to values which are thought to be nearly exact. The exponent ν is found[7] as $\nu = 0.59$, which is the value we will use in what follows. Scaling functions have not been calculated in such detail. However, both for phase transitions and for polymer solutions it is found that a first-order or second-order calculation in general fits the experimental data.

Recently, Knoll, Witten, and the present author have undertaken a detailed second-order calculation of the

0024-9297/82/2215-0652$01.25/0

thermodynamic scaling functional $\mathcal{P}$ in the excluded volume limit, including the first-order polydispersity dependence and covering the full range of overlap s from the dilute regime $s \to 0$ to the semidilute regime $s \to \infty$. This calculation is quite involved and has been published elsewhere.[8] It is the purpose of the present paper to present our results to polymer physicists who may not be interested in the details of a renormalization group calculation and to compare our results with previous theories and with experiments. In keeping with the general trend, we find that our calculation adequately reproduces the universal behavior of the osmotic pressure data over the whole range of overlap. For small overlap it supports the analysis of data via a "square root plot", though it also reveals that virial coefficients extracted by this method are effective parameters rather than true expansion coefficients. The polydispersity dependence is found to be weak and opposite to that predicted by other theories. This being a point of major concern to us, we again analyzed the experimental information on the polydispersity dependence of the second virial coefficient A_2. We find that the virial coefficients, as extracted in the relevant references,[9,28] show a general trend which suggests that they are effective parameters depending on the method used in the data analysis. We show that their interpretation as true virial coefficients is inconsistent and that our theory allows for a consistent interpretation of most data. However, the experimental uncertainty, as measured by random deviations from the strong results of scaling and universality, is too big to draw any firm conclusions.

The organization of this article is as follows. In section 2 we analyze experimental data to extract the universal scaling function. We present the result of our calculation and compare it with experiment and with previous theoretical calculations. We also discuss the limits of applicability of our result. Section 3 is devoted to a discussion of the second virial coefficient and its polydispersity dependence. A résumé is contained in section 4.

2. Thermodynamic Scaling Function for Arbitrary Overlap

2.1. Experimental Results for the Universal Scaling Function. We first extract the universal scaling function from the available experimental data. To check that the data indeed obey scaling we have to analyze experiments on a single polymer–solvent system at a fixed temperature but for fractions of very different chain lengths. The data of Fox et al.[11] on poly(methyl methacrylate) (PMMA) in acetone serve that purpose very well. In Figure 1 we plot their results for $\mathcal{P} = \Pi/RTc_p - 1$ as function of the scaling variable $s = bc_pN^{3\nu}$. The value of b is of no importance for the present discussion, but N has been redetermined for each fraction in such a way that the data fit a common curve as well as possible. The values of N determined in this way do not differ much from the values given in the original work (see Table I). To avoid polydispersity effects we used only the results for sharp fractions (M_w/M_n from 1.2 to 1.3). Also included in the plot are data of Kuwahara et al.[12] on the same system. It is obvious that these data, which span more than an order of magnitude in chain length N, confirm the scaling behavior. Within the experimental error they fall on a common curve. [The curve given in Figure 1 is the result of our calculation as will be discussed in subsection 2.3]. This simple scaling behavior proves that the excluded volume limit $z \gg 1$ has been reached for this system. Outside that limit the N dependence of $\mathcal{P}$ is not contained in the single scaling variable s only but is also due to a change of z. This would show up in Figure 1 by the impossibility of fitting the data for different fractions to the same curve.

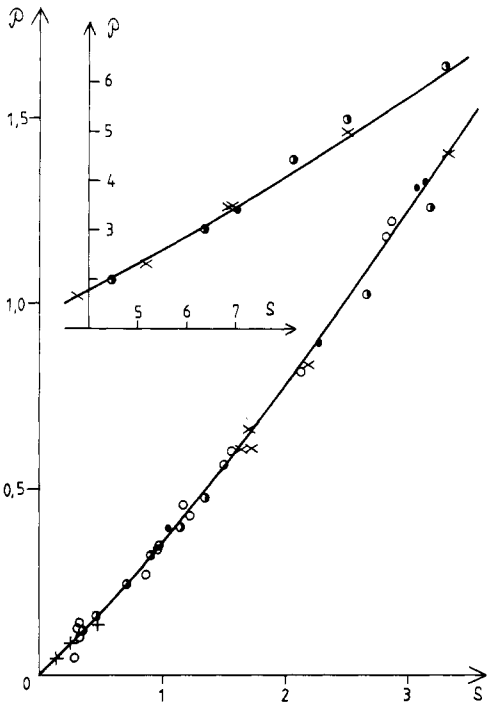

Figure 1. Scaling function $\mathcal{P}$ vs. s for PMMA–acetone. The data points are taken from the following experiments: (◑) ref 12, N = 1615; (+) ref 11, N = 652; (○) N = 1660; (●) N = 2848; (×) N = 8330. N values are taken from the fit to the theoretical curve.

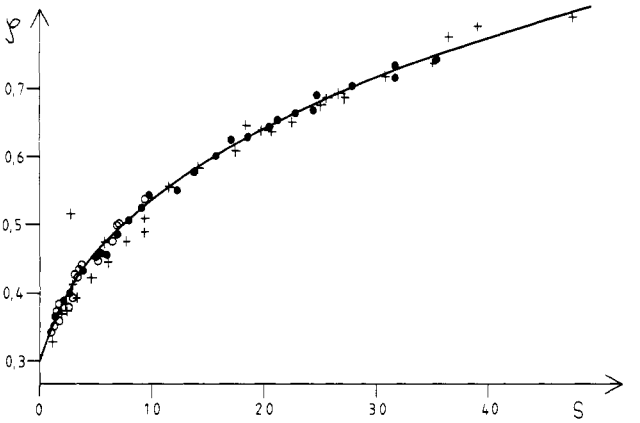

Figure 2. Effective second virial coefficient ρ vs. s. Data points: (○) PMMA–acetone, ref 11, N = 8330; (●) PDMS–cyclohexane, ref 13, N = 1745; (+) PS–toluene, ref 14, N = 1320, and ref 15, N = 4900. The curve is calculated from our theory.

Having established the scaling behavior, we check the other strong result, namely, the universality of the functional $\mathcal{P}$. In Figure 2 we have plotted the "effective second virial coefficient"

$$\rho(s) = \left(\frac{\Pi}{RTc_p} - 1\right)s^{-1} \equiv s^{-1}\mathcal{P}(s,p(y)) \qquad (2.1)$$

as function of the overlap for the three chemically different systems PMMA–acetone,[11] poly(dimethylsiloxane) (PDMS)–cyclohexane,[13] and polystyrene (PS)–toluene.[14,15] The parameter b for each system has been determined in such a way that the data fall on a common curve. For the PS system, data at two different temperatures, T = 30 °C[14] and T = 27 °C,[15] have been used. Plotting $\rho(s)$ we have eliminated the linear increase of $\mathcal{P}$ and we concentrate on the more interesting deviations from this trivial behavior. The price paid for that advantage is a strong magnification

Table I
Experiments Which Have Been Fitted to Our Theory[a]

system	T, °C	"N"	10^{-4}"Γ_2"	b	N	$10^{-4}\Gamma_2$	ref	remarks
PS-toluene	30	1270	0.62	82.7	1320	0.65	14	Figure 2
	27	5027	2.8	83.7	4900	1.7	15	Figure 2
	69.2	5027	2.1	81.5	5400	1.8	15	
PDMS-cyclohexane	20	1640	0.47	50.9	1745	0.48	13	Figure 2
	20	6510	1.39	50.2	6530	1.32	13	
	20	6640	1.39	51.8	6860	1.41	13	
PDMS-toluene	20	1370	0.27	31.6	1360	0.25	13	
	20	2880	0.50	34.4	3220	0.52	13	few points
PDMS-hexane	20	1850-1950	not given	59	2150	0.65	19	first 9 points
	50	1850-1950	not given	52	2150	0.57	19	few points
PDMS-heptane	35	1850-1950	not given	50	2300	0.58	19	Figure 5, first 5 points
	50	1850-1950	not given	45	2300	0.52	19	Figure 5, first 5 points
PDMS-octane	20	1850-1950	not given	39	2300	0.45	19	Figure 5, first 5 points
	35	1850-1950	not given	42	1900	0.42	19	first 5 points
	50	1850-1950	not given	46	2200	0.52	19	first 5 points
PDMS-nonane	50	1850-1950	not given	37	2200	0.42	19	first 4 points
PMMA-acetone	30	1608	0.30	31.8	1608	0.28	12	Figures 1 and 5, first 14 points
	30	660	0.15	31.8	652	0.14	11	Figure 1
	30	1660	0.33	31.8	1660	0.29	11	low precision, Figure 1
	30	2780	0.46	31.8	2848	0.44	11	Figure 1
	30	4020	0.61	31.8	4250	0.59	11	$M_w/M_n = 2$
	30	7260	0.95	31.8	8330	1.01	11	Figures 1 and 2
PMMA-toluene	30	3820	0.61	44.9	4300	0.85	11	
poly(α-methyl-styrene)-toluene	25	1690	not given	90	1740	0.87	29	the different values of b are found for different measuring devices
	25	4280	not given	90	4650	1.86	29	
	25	1690[b]	not given	83.5	1740	0.81	29	
	25	10070[c]	not given	83.5	12800	3.76	29	
	25	15400	not given	83.5	17000	4.68	29	

[a] The rows "N" and 10^{-4}"Γ_2" present the values given in the literature. N and $10^{-4}\Gamma_2$ are taken from our analysis. 10^{-4}"Γ_2", b, and $10^{-4}\Gamma_2$ are in units of cm³/mol. In some cases the experimental range extended to high concentrations, permitting the use of only the first few data points. [b] Fraction B of ref 28. [c] Fraction C of ref 28.

of the experimental error for small overlap. We therefore have not included data for $s < 1$.

It is obvious that the data follow a common law. We have to make sure that this law indeed represents the universal excluded volume limit. One way to show this is to check whether the data for a given chemical system and temperature obey the scaling dependence on N. Above, this has been shown for the PMMA–acetone system. For the other systems we find similar results. Thus, since all three systems consist of long molecules in very good solvents and since all three systems show simple scaling behavior as a function of N, *we conclude that Figure 2 represents the experimentally determined universal scaling function for the effective second virial coefficient.* If significant deviations from this curve should occur for other systems, they must be traced back to a violation of the excluded volume limit. This will be discussed in more detail in subsection 2.3.

2.2. Results of the Renormalization Group Calculation. In ref 8 we have calculated the scaling functional $\mathcal{P}(s,p(y))$ by a method which in renormalization group theory is known as ϵ expansion and which for polymer physicists can be characterized as a "renormalized" cluster expansion. One of the main differences from the cluster expansion as reviewed in section III.14 of Yamakawa's book[6] is that the "bare" interaction parameter $z = \beta N^{1/2}$ is replaced by a renormalized parameter g^* which contains contributions from an infinite set of cluster diagrams and which can be shown to stay finite and small as z tends to infinity. Thus it can be hoped that a low-order expansion in this new parameter will give reasonable results also in the excluded volume limit $z \to \infty$. We have carried this expansion to the second order. In first order we included the effect of polydispersity, whereas the second order was calculated only for the equilibrium ensemble which up to small corrections is characterized by an exponential chain length distribution $p(y) = \exp(-y)$. Calculation of $\mathcal{P}$ for arbitrary overlap was possible only via a "RPA-type" resummation of cluster diagrams; i.e., we have to consider configurations in which a given chain interacts with itself via an intermediate sequence of any number of other chains. A systematic and consistent procedure to deal with such configurations has been developed and the details can be found in ref 8 and 16.

The precise form of our result is complicated since it can only be given in terms of a parameter representation $\mathcal{P}(s,p(y)) = \tilde{\mathcal{P}}(w,p(y))$, $s = \tilde{s}(w,p(y))$, where the last equation cannot be solved analytically to get $w = \tilde{w}(s,p(y))$. However, we can construct an approximate form, reproducing the full result for all s within deviations of less than 1%.

$$\mathcal{P}(s,p(y)) = \frac{s}{4}\left[\frac{40 + 27s + s^2}{22 + s}\right]^{0.30} C(s,p(y)) \quad (2.2)$$

$$C(s,p(y)) = 1 + 0.06\left(2 - \frac{M_w}{M_n}\right)(0.68)^s \quad (2.3)$$

The full results can be found in eq 3.21 and 3.22 and eq 4.14 and 4.15 of ref 8. As mentioned above, the polydispersity correction $C(s,p(y))$ given here is based on a first-order calculation whereas the other factor on the right-hand side of eq 2.2 is fitted to the results of a second-order calculation for the equilibrium ensemble, where $M_w = 2M_n$ is a good approximation. We stress that eq 2.2 and 2.3 just represent a convenient way to reproduce our results numerically within the accuracy of a second-order calculation. The precise analytical form of these expressions is not relevant. Especially we have chosen to parametrize the polydispersity dependence in the simplest way possible, and since this dependence is small, the rough characterization of $p(y)$ in terms of M_w/M_n is adequate for all but very special chain length distributions. For in-

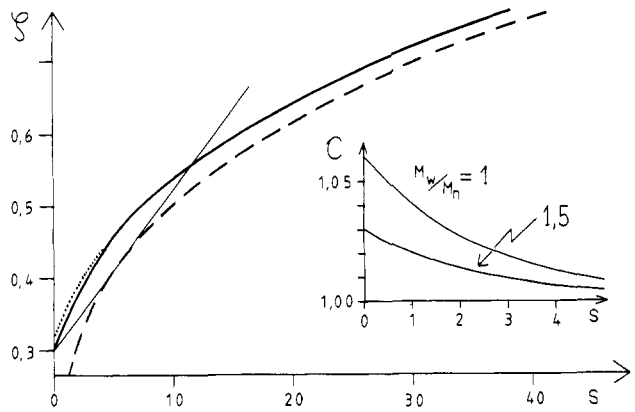

Figure 3. Effective second virial coefficient ρ vs. s, as calculated from our theory. The full curve gives ρ for $M_w/M_n = 2$. The dotted curve for $s < 5$ gives the monodisperse result ($M_w/M_n = 1$). The broken curve represents the asymptotic law, and the straight line represents the square root plot. The insert gives the polydispersity correction $C(s,p(y))$ for two different values of M_w/M_n.

stance, it may not be adequate for a mixture of two sharp fractions of widely different molecular weight, and in section 3 we will present our results for the true second virial coefficient A_2, including the full dependence on $p(y)$.

Equations 2.2 and 2.3 reproduce the known exact behavior of $\mathcal{P}$ for large overlap

$$\mathcal{P}(s,p(y)) \underset{s\to\infty}{\to} \text{const} \times s^{1/(3\nu-1)} = \text{const} \times s^{1.30} \quad (2.4)$$

This behavior is independent of polydispersity. It was first derived by des Cloizeaux[2] using the intuitively obvious assumption that Π/RT for large overlap should depend only on the weight concentration c_pN of polymer in the solution. On a more rigorous level eq 2.4 can be shown to be an immediate consequence of the structure of the parameter representation derived in ref 8. Since the asymptotic behavior is independent of polydispersity, it is well suited for fixing the nonuniversal, but polydispersity-independent, scale factor b contained in s (eq 1.2). This factor is an arbitrary scale of the theory, which has to be fixed by a normalization condition. *We choose b such that the value of the constant in eq 2.4 is* $^1/_4$, which happens to be the value found in a lowest order calculation in terms of renormalized variables (compare eq 3.24 of ref 8).

In Figure 3 we present the results (2.2) and (2.3) for $\rho = \mathcal{P}(s,p(y))/s$. It is seen that the polydispersity dependence vanishes rapidly with increasing s. For $s \gtrsim 4$, $\rho(s,p(y))$ is almost independent of polydisperisty. We have also given the asymptotic form $\rho \sim {}^1/_4 s^{0.30}$. The overall shape of the exact curve is remarkably similar to the asymptotic law, but the corrections to the asymptotic behavior are not negligible even for fairly large values, $s \simeq 50$. This is in keeping with the experimental results as given in Figure 1 of ref 17. [Since we could not obtain a tabulation of the data, we, unfortunately, are not able to include these measurements in our quantitative analysis.]

A rough idea of the accuracy of the theoretical result can be taken from the size of the second-order correction. For the asymptotically normalized form it is found that this correction nowhere exceeds 8%. We therefore estimate the overall accuracy of our result to be of the order of a few percent. To illustrate this statement we give the numerical value of the universal ratio R_Π which can be constructed from the second virial coefficient and the coefficient of the asymptotic power of s:

$$R_\Pi[p(y)] = \rho^{-1}(0,p(y))[\lim_{s\to\infty} \mathcal{P}(s,p(y))s^{1/(1-3\nu)}]^{3\nu-1} \quad (2.5)$$

This ratio characterizes the overall shape of $\rho(s,p(y))$. In the equilibrium ensemble we find the values

$$R_\Pi^e = 1.00 \text{ to zero order}$$
$$R_\Pi^e = 1.22 \text{ to first order} \quad (2.6)$$
$$R_\Pi^e = 1.28 \text{ to second order}$$

In the discussion to follow, a ratio characterizing the small overlap behavior is of some interest, too. Considering the Taylor expansion of $\mathcal{P}(s,p(y))$

$$\mathcal{P}(s,p(y)) = A_2[p(y)]s + A_3[p(y)]s^2 + \ldots \quad (2.7)$$

we note that any combination of the terms of this series in which s drops out is universal. In particular we can define a universal ratio

$$\alpha[p(y)] = A_3[p(y)]/A_2^2[p(y)] \quad (2.8)$$

This ratio is identical with the ratio of the corresponding virial coefficients of the osmotic pressure defined according to Stockmayer and Casassa.[18]

$$\frac{\Pi}{RTc_pN} = \frac{1}{N}(1 + \Gamma_2 c_pN + \Gamma_3(c_pN)^2 + \ldots) \quad (2.9)$$

Equations 1.5, 1.2, 2.8, and 2.9 yield the relations

$$\Gamma_2 = bN^{3\nu-1}A_2[p(y)] \quad (2.10a)$$
$$\Gamma_3 = b^2N^{6\nu-2}A_3[p(y)] \quad (2.10b)$$

which lead to

$$\Gamma_3\Gamma_2^{-2} = \alpha[p(y)] \quad (2.11)$$

For the equilibrium ensemble the results for α first have been given by des Cloizeaux[2]

$$\alpha^e = 0.67 \text{ to first order}$$
$$\alpha^e = 0.36 \text{ to second order} \quad (2.12a)$$

For the monodisperse ensemble we find[8]

$$\alpha^m = 0.44 \text{ to first order} \quad (2.12b)$$

We note that this ratio is very sensitive both to polydispersity effects and to higher order corrections, quite in contrast to the overall form of our results. The reason is easily understood. Since the asymptotic form of $\mathcal{P}(s,p(y))$ is independent of polydispersity, the polydispersity corrections to A_2 and A_3 always go in opposite directions. If A_2 is increased, A_3 has to decrease for the curve to approach smoothly the same asymptotic form, and vice versa. Thus in the combination $\alpha[p(y)]$ corrections to A_3 and A_2 add up. Furthermore, second-order corrections to A_3 are a larger percentage of the value of A_3 since in such a higher virial coefficient the zeroth order vanishes.

2.3. Comparison with Experiment and with Previous Theories. The curves drawn in Figures 1 and 2 are calculated according to our theory. In Figure 1 we choose $M_w/M_n = 1.2$, whereas in Figure 2 we neglected the weak polydispersity dependence, setting $C(s,p(y)) = 1$ (i.e., $M_w/M_n = 2$). Obviously, theory and experiment agree within the experimental uncertainty. We have checked all the data which we could find, and in most cases (see Table I for a compilation) we have found full agreement between theory and experiment. A few exceptions will be discussed below. The experiments evaluated in Figures 1 or 2 are those which cover a particularly large range of N or s. For most experiments the range of s is too small to show the curvature of $\rho(s,p(y))$.

Universality tells us that the excluded volume limit contains very little information on the properties of the solution under investigation. Besides the chain length N

(and the distribution function $p(y)$) it is only the parameter b which is specific for the system. This parameter cannot be calculated from the renormalization group, but a systematic study of a variety of solutions at a variety of temperatures might lead to a phenomenological theory. The set of systems which we have fitted is not rich enough to allow for such an analysis. Still, some remarks giving a feeling for the size of b may be appropriate. From an inspection of the theory it is found that b takes the form $b = {}^2/_3 g N_A B^3$, where N_A is Avogadro's number, g is a dimensionless interaction constant which takes a fixed value $g \simeq 3\pi^2/2$, and B is a length which can be interpreted as the effective size of a monomer. Using the typical value $b \simeq 50$ cm^3/mol, we find $B \simeq 2 \times 10^{-8}$ cm, which is a reasonable microscopic length scale. Another way to get a feeling for our parameter is to note that the radius of gyration of an isolated chain to lowest order is found as $R = BN^\nu$.

In most experiments the chain length N itself is not determined independently but is deduced from an analysis of the osmotic pressure data. We therefore used N as a parameter in our fit. As shown in Table I our values of N, in general, do not differ significantly from the values given in the literature. A priori this is somewhat surprising, for the following reason: Using $R \simeq BN^\nu$, we can estimate the value of s where the chains start to overlap. We find $s \simeq 2.5$, and thus most experimental values for larger chains ($N \geq 1500$) are taken in a regime where the chains are not isolated. The extraction of N from such data could show a large systematic error. The explanation for the good agreement between the old and the new values of N is found by reconsidering the way in which the data have been analyzed in the literature. Nearly all references used a "square root plot". $(\Pi/RTc_pN)^{1/2}$ was plotted as function of c_pN and the result was fitted to the linear form $N^{-1/2}(1 + 1/2\Gamma_2 c_p N)$. In the virial expansion (2.9) this amounts to the neglect of all terms beyond third order and to the choice $\alpha[p(y)] = {}^1/_4$. The corresponding curve is included in Figure 3. Obviously, this on the average gives an adequate representation of $\rho(s,p(y))$ for $s < 15$. It underestimates A_3, but this is compensated by the neglect of higher virial coefficients. The coupling of A_3 to A_2 inherent in the method makes it very sensitive to a deviation in A_2. Increasing A_2 we also increase the slope of the square root plot, and thus the deviation from our theoretical curve increases rapidly.

To illustrate these considerations we have determined the parameters of the square root plot passing through two theoretical points $(s, \Pi/RTc_p)$ at $s = 1$ and $s = 10$ for a system with $N = 1000$, $b = 50$ cm^3/mol, and $A_2 = 0.3$ cm^3/mol, for which a theoretical value $\Gamma_2 = 3110$ cm^3/mol follows. The square root plot yields $N = 984$ and $\Gamma_3 = 3080$ cm^3/mol. The agreement becomes worse if the experiments do not cover the region of small s. For instance, substituting the point $s = 1$ by the point $s = 2$ in the above calculation, we find $N = 950$, $\Gamma_2 = 2980$ cm^3/mol, and $A_2 = 0.305$ cm^3/mol. Since with increasing N the range of s covered by an experiment usually shifts to higher values, this suggests that the square root plot systematically underestimates the larger chain lengths. This is supported by the results given in Table I, and it is illustrated by curves B and C of Figure 8. It is interesting to note that by virtue of the coupling between Γ_2 and Γ_3 the square root plot in general is superior to an analysis which uses N, Γ_2, and Γ_3 as *independent* parameters. Applying such an analysis to three points in the intervall $1 < s < 10$, we find completely wrong values. This observation is supported by the analysis contained in ref 28.

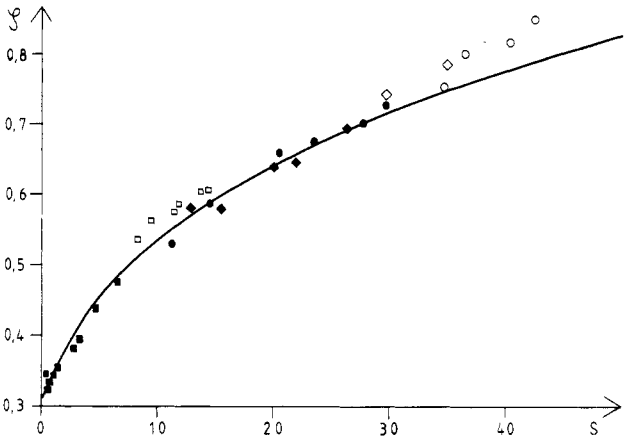

Figure 4. $\rho(s,p(y))$ from measurements extending to high concentrations. Reference 19, PDMS–octane, $T = 20$ °C, weight fraction $w_2 < 0.2$ (●); $w_2 > 0.2$ (○). PDMS–heptane, $T = 50$ °C, $w_2 < 0.2$ (♦); $w_2 > 0.2$ (◇). Reference 12, PMMA–acetone, $w_2 < 0.15$ (■); $w_2 > 0.15$ (□).

All this discussion shows that the "virial coefficients" Γ_K usually extracted from experiment are effective parameters characterizing $\rho(s,p(y))$ in an intermediate s range rather than exact virial coefficients of a Taylor expansion around $s = 0$. Indeed, analyzing our analytical results[8] via the rigorous Taylor expansion, we find that we have to include many orders to go beyond $s \simeq 5$. This is due to the fact that the expansion then has to simulate the power dependence $\rho \sim s^{0.30}$, which does not allow for a Taylor expansion.

We next consider the limitations of our approach. Since the theory is restricted to weak solutions, we expect to find deviations for larger concentrations. The concentration where the theory breaks down will depend on the special system under investigation and cannot be predicted from our theory. Empirically we have found that for most systems the theory fits the data up to polymer weight fraction of about 0.15–0.20, which are surprisingly large values. Above this concentration the experimental values seem to increase more strongly than the theoretical curve. This is a reasonable behavior, and it is illustrated in Figure 4 with data taken from ref 12 and 19.

Our results also are not applicable if the chains become too short or if the solvent is not good enough. Both effects in principle can be taken care of by calculating the scaling functional as a function of both scaling variables s and $z = \beta N^{1/2}$. Both effects are expected to decrease the slope of $\rho(s,p(y))$, thus diminishing the ratio $\alpha = A_3/A_2^2$. Qualitatively, this behavior can clearly be seen, for instance, from Figure 3 of ref 13, where $\rho(s,p(y))$ is plotted for PDMS in three different solvents. We have not been able to find data which show this effect as a function of N. All we can seay is that even the shortest chains we have analyzed ($N \simeq 600$) in good solvents are still in the excluded volume limit. It needs more accurate measurements for shorter chains to find significant deviations.

To finish our comparison to experiment we want to mention data which cannot be fit by our theory. In particular, the experiments of ref 20 show a structure in $\rho(s,p(y))$ which is absent in our results. If that structure is real, it would amount to a serious deviation from universality which we cannot explain. Also the results of ref 12 on the PMMA–benzene system do not fit to our theory. We can deal with these data only if we assume that for that system corrections due to $c_pN \neq 0$ set in even at polymer weight fractions less than 0.05.

Most of the previous theoretical work has been restricted either to large concentrations (weight fractions above 20%)

or to a calculation of the second or third virial coefficient. An exception is given by the work of Fixman.[21] This goes beyond the present work in that it allows for a change of the parameters with increasing concentration. However, the basic approach is clearly less reliable, since it is based on a rough ansatz for the potential energy of two chains in solution. Fixman's result differs from ours in that the curvature of ρ as a function of c_pN is much larger. It therefore does not fit the universal curve $\rho(s,p(y))$ extracted in Figure 2, but it does fit the experiments of ref 20. Theories of the second virial coefficient have been reviewed by Yamakawa (see ref 6, section 21). Partly these theories contradict our theory in that they do not predict a finite limit for $A_2 \sim \Gamma_2 N^{1-3\nu}$ (compare eq 2.10a) as z tends to infinity. But even those theories which yield a finite excluded volume limit are not consistent with our results. They in general predict that the excluded volume limit has not yet been obtained in the measurements analyzed here. This is clearly shown by the analysis of ref 22, and it has been observed before in the context of a discussion of the interpenetration ratio.[23]

3. Second Virial Coefficient

From the analysis of the previous section we know that it is difficult to extract reliable values of the true second virial coefficient from the experimental data without using theoretical information about the function $\rho(s,p(y))$. This greatly diminishes the value of a detailed study of this coefficient. Still, the coefficient contains the dominant polydispersity dependence of the osmotic pressure, which makes an analysis interesting. We first note some strong results of the renormalization group, formulated in terms of the coefficient $A_2[p(y)]$ defined in eq 2.7.

As is well-known,[6] the polydispersity dependence of $A_2[p(y)]$ takes the form

$$A_2[p(y)] = \int_0^\infty dy\, dy'\, p(y)p(y')a_2(y,y') \qquad (3.1)$$

The function $a_2(y,y')$ also determines the virial coefficient for light scattering:

$$A_2^{l}[p(y)] = \left(\int_0^\infty dy\, p(y)y^2\right)^{-2} \int_0^\infty dy\, dy'\, yy'p(y)p(y')a_2(y,y') \qquad (3.2)$$

We recall that $p(y)$ is the reduced chain length distribution defined in eq 1.3 in terms of the probability $P(n)$ to find a chain of $n = yN$ monomers. $p(y)$ is normalized according to the conditions

$$\int_0^\infty dy\, p(y) = 1 = \int_0^\infty dy\, yp(y) \qquad (3.3)$$

For the set of Schultz distributions it takes the form

$$p_\sigma(y) = \frac{\sigma}{\Gamma(\sigma)}(\sigma y)^{\sigma-1}e^{-\sigma y} \qquad (3.4)$$

where $\Gamma(\sigma)$ denotes the Gamma function. If we combine the scaling law for Π/RT with the representation (3.1) of A_2, we find a homogeneity relation for $a_2(y,y')$:

$$a_2(y,y') = \lambda^{-3\nu}a_2(\lambda y,\lambda y') \qquad \lambda > 0 \qquad (3.5)$$

Since A_2 is multiplied by the arbitrary scale b, the function $a_2(y,y')$ is not universal. However, universality holds for any ratio, for instance, for the expression $a_2(y,y')/a_2(1,1)$.

Our calculation yields $a_2(y,y')$ in first order. We find[8]

$$a_2(y,y') = \tfrac{1}{2}A_0[4(yy')^{3/2\nu} + y^{3\nu} + y'^{3\nu} - (y + y')^{3\nu}] \qquad (3.6)$$

where with our normalization A_0 takes the value 0.31. Some remarks about the form (3.6) are necessary. Our method does not yield eq 3.6 directly but rather an expression involving logarithms which can be interpreted as first terms in the expansion of $y^{3\nu-2} = \exp|(3\nu - 2) \ln y|$. These logarithms have to be exponentiated in a form consistent with the scaling law (3.5). This fixes the form of $a_2(y,y')$ partly, but not completely. The remaining ambiguity can be eliminated only by a theory which gives $a_2(y,y')$ for an extreme ratio of the arguments: $y/y' \to 0$ or ∞. However, within reasonable limits [$0.02 < y/y' < 50$] this ambiguity is of no numerical importance.

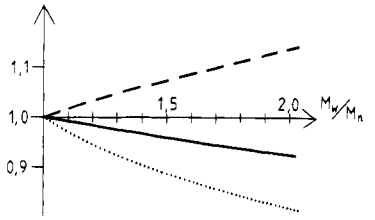

Figure 5. Second virial coefficients for Schultz distributions as a function of M_w/M_n: full curve, $A_2[p_\sigma(y)]/A_2$ (monodisperse) from our calculation; dotted curve, same ratio for the light scattering virial coefficients; broken curve, same ratio for osmotic pressure virial coefficients according to Casassa's calculation.

Using the form (3.6), we have evaluated the second virial coefficients for the Schultz distributions. We find

$$A_2[p_\sigma(y)] = \frac{1}{2}A_0\sigma^{-3\nu}\left[4\left(\frac{\Gamma(\sigma + {}^3/_2\nu)}{\Gamma(\sigma)}\right)^2 + 2\frac{\Gamma(\sigma + 3\nu)}{\Gamma(\sigma)} - \frac{\Gamma(2\sigma + 3\nu)}{\Gamma(2\sigma)}\right] \qquad (3.7)$$

$$A_2^{l}[p_\sigma(y)] = \left(\frac{\sigma}{1 + \sigma}\right)^{2-3\nu} A_2[p_{\sigma+1}(y)] \qquad (3.8)$$

the latter relation being true generally for Schultz distributions. In Figure 5 we plot these results as function of $M_w/M_n = 1 + 1/\sigma$. Also given are results from Casassa's theory,[24] which in our notation is based on the expression

$$a_2^{C}(y,y') = A_1(y^\nu + y'^\nu)^3 \qquad (3.9)$$

[In casassa's work the exponent ν in expression 3.9 is an empirical parameter. Here, the scaling law (3.5) identifies this parameter as the excluded volume exponent.] It is seen that our results disagree with those of Casassa even in the sign of the effect, the only reward being that the effect is small according to both theories. In particular, it is within the error bars of a normal experiment as can be seen, for instance, from ref 11, where no systematic effect of polydispersity on A_2 has been found.

However, there exist specific experiments designed to test the polydispersity dependence of A_2 or A_2^{l}. These experiments use mixtures of two sharp fractions which differ in molecular weight by an order of magnitude. Of the data available[9,10,25,26,28,30-33] we cannot use the results of ref 25, 30, and 31. In ref 25 a polymer-solvent system near its Θ temperature was examined, whereas the mixtures used in ref 30 and 31 contain a component of very short chain length. To analyze these data we have to go beyond the excluded volume limit, extending our theory to finite values of z. The work of ref 26 was inconclusive, as has been discussed by Casassa.[27] We here reconsider the remaining experimental evidence.

As first pointed out by Casassa[27] the data on mixtures of sharp fractions of chain lengths n_1 and n_2 are best analyzed in terms of the virial coefficients of the sharp fractions and the virial coefficient of two chains of different length. We here use $a_2(y_i,y_i)$, $i = 1, 2$, and $a_2(y_1,y_2)$, where

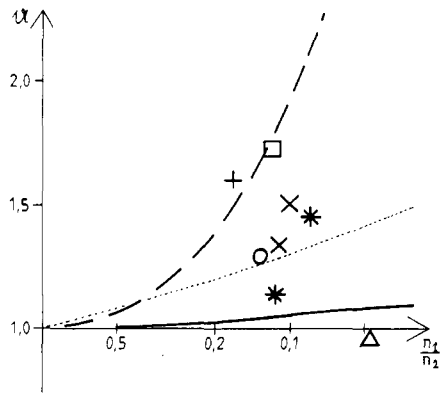

Figure 6. Universal function $a(n_1/n_2)$ according to our calculation (full line) and to Casassa's calculation (broken line). The dotted line separates the region where a maximum of A_2 is found (above) from the region where no such maximum occurs (below). Experimental results: (×) ref 9; (△) ref 10; (*) ref 26; (□) ref 33; as evaluated by Cassasa,[27] Table I. Further experiments: (○) ref 32; (+) ref 28.

$y_i = n_i/N$. From these coefficients we can construct a universal function

$$a\left(\frac{n_1}{n_2}\right) = \frac{a_2(y_1,y_2)}{[a_2(y_1,y_1)a_2(y_2,y_2)]^{1/2}} \qquad (3.10)$$

where we have used the scaling law (3.5) to show that this function depends only on $y_1/y_2 = n_1/n_2$. In Figure 6 we have plotted $a(x)$ evaluated according to our result (3.6) as well as according to Casassa's theory (3.9). We also have given the experimental data of ref 9, 10, 26, 28, and 32. It is obvious that these data do not fit a universal curve; i.e., they violate a strong statement which is independent of the specific calculation of $a(x)$. We therefore reconsider the data more closely, concentrating on the measurements[9,28] of the osmotic pressure. [The extraction of A_2 from light scattering experiments[10,32,33] involves an extrapolation to zero scattering angle. We therefore can reanalyze these data only after we have calculated the scaling function for the scattering intensity.] Of the work of Noda et al.[28] we use only the data for mixtures of fractions B and C. Fraction A is too short for an application of our theory.

In the evaluation of their data both Flory and Krigbaum[9] and Noda et al.[28] used the first virial coefficient M_n^{-1} as a fit parameter. In most cases the so-determined average molecular weight M_n^{exptl} of the mixtures differs from the molecular weight M_n^{calcd} calculated from M_n^{exptl} of the pure fractions, but this difference is not thought to be significant. However, a closer inspection reveals that the deviations of M_n^{exptl} are correlated with the behavior of A_2. Large values of A_2 are associated with small values of M_n^{calcd}/M_n^{exptl}, and vice versa. A maximum of A_2 as function of the composition reflects itself as a minimum of M_n^{calcd}/M_n^{exptl}. This correlation holds generally, even outside the excluded volume limit. The system polyisobutylene–cyclohexane[9] is an exception to that rule, but in that case the maximum of A_2 is not very pronounced and the number of data points is very small.

This observation suggests that the experimental virial coefficients $(M_n^{exptl})^{-1}$ and A_2 are effective parameters valid for the experimental concentration range. Since these parameters are correlated and since one of these parameters $[(M_n^{exptl})^{-1}]$ differs from its known exact value, so will the other. This is illustrated in Figure 7 for the PS–toluene data of Flory and Krigbaum. Taking the values of Γ_2 and M_n as quoted by the authors, we have calculated A_2 with the help of eq 2.10a. [The value of b has been taken from Table I]. The result is plotted in Figure 7a. We note that

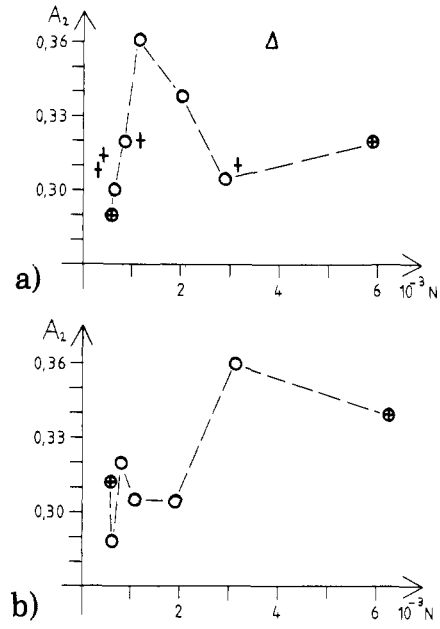

Figure 7. Values of A_2 for PS–toluene. (a) Values as calculated from the results for Γ_2, N given in ref 9. Crosses denote sharp fractions, the triangle represents a polydisperse fraction, and circles denote mixtures of the two sharp fractions given as crossed circles. The line serves to guide the eye. (b) Values as determined from the mixture data with corrected values of N.

even the data for the sharp fractions scatter widely: nevertheless, there is a definite maximum in the data for the mixtures. We then have redetermined the chain lengths by a least-squares fit using the measured lengths and the concentrations as input and the lengths of the sharp fractions as fit parameters. For each fraction the value of M_n thus determined has been used in a square root plot for the determination of A_2. The result is given as Figure 7b, which shows that the maximum has vanished. This clearly shows that *the maximum cannot be interpreted consistently as a feature of the true second virial coefficient* but is a property of an effective virial coefficient which depends on the method used to analyze the data.

Analyzing the data with the help of our theory, we find that the experimental error in the data of Flory and Krigbaum is too large for a detailed discussion, whereas the data of Nodal et al. can be consistently explained by our theory. In Figure 8 we present a square root plot for the data on the B–C mixtures. The theoretical curves have been calculated by adjusting the parameters as follows: The nonuniversal parameter b and the chain lengths of fractions B and C have been determined by fitting the data to eq 2.2, taking $M_w/M_n = 1$. The parameter b in addition allows for a consistent fit of all the other data[29] for the poly(α-methylstyrene)–toluene system taken with the same experimental equipment (compare the remark in Table I). With all parameters fixed the curves for the mixtures have been calculated from eq 2.2, ignoring the polydispersity dependence. Obviously, the theoretical curves reproduce the data quite well. According to our theory, the polydispersity correction will diminish the initial slope of curves BC-1 to BC-5 by at most 5%; it will decrease $[10^3\Pi/RTc_e]^{1/2}$ by less than 0.01. Clearly, such an effect is within the error of the experiment. *We thus conclude that these data can be consistently interpreted by our theory. Polydispersity effects are too small to be identified.* We want to mention one weak point of our analysis. In fitting the data of fraction C, we have used an optimal chain length $N = 1.28 \times 10^4$, whereas independent light scattering or osmotic pressure measurements[34] on the same

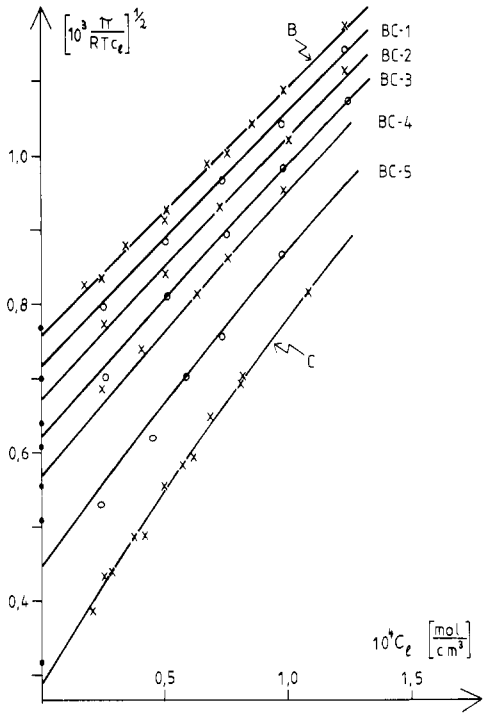

Figure 8. Square root plot for mixtures of sharp fractions of poly(α-methylstyrene) in toluene.[28] Fraction B, $N = 1730$; fraction C, $N = 12\,800$. Weight fractions of component C: BC-1, 0.125; BC-2, 0.254; BC-3, 0.378; BC-4, 0.500; BC-5, 0.751. The curves are calculated according to our theory. The heavy dots are calculated from the molecular weights as evaluated in ref 28. Crosses (circles) represent data for fractions B, BC-2, BC-4, and C (BC-1, BC-3, and BC-5). $c_1 = c_p N$ denotes the monomer concentration.

sample (in ref 34 denoted by PαS-9) yield $N = 1.01 \times 10^4$. If evaluated with this smaller value of N, the data for fraction C show a systematic deviation from the well-established universal function $\mathcal{P}(s,p(y))$, and the increase of N according to our evaluation is consistent with the general remarks in subsection 2.3.

In the absence of reliable experimental information on the polydispersity dependence we reconsider the theoretical arguments. We have stressed above that we cannot determine the analytic structure of $a_2(y,y')$ uniquely; we, however, can check whether the form (3.9) is compatible with our first-order result. It is found that this is not the case, and thus this form cannot be the correct result. [Indeed, as stressed above, for $0.02 < y/y' < 50$ our first-order result numerically is unambiguous.] However, it still might be a reasonable approximation to a full calculation including higher order effects. Equation 3.9 was derived from the assumption that a chain of length n behaves like a hard sphere of radius $R(n) \sim n^\nu$. This assumption may be motivated by the fact that the relation between the third and the second virial coefficient follows a "hard-sphere law": $\Gamma_3 \sim \Gamma_2^2$. However, this analogy is misleading. The relation $\Gamma_3 \sim \Gamma_2^2$ is a consequence of the fact that the system posseses only a single macroscopic length scale. Taking this scale to be given by the average radius R of a chain, we find that a dimensionless function like $\mathcal{P}$ necessarily must depend on the dimensionless combination $R^3 c_p$ of R and c_p, which immediately yields the scaling result $\Gamma_3 \sim \Gamma_2^2$. The analogy to hard spheres is valid only insofar as hard spheres also possess only a single length scale.

Having argued against the hard-sphere analogy, we propose another picture which favors the qualitative form of our result. Our point is that a chain in solution, rather than being characterized as "hard" or "soft", should be characterized as "loose". It is well-known that the average density of monomers inside an isolated coil decreases rapidly with increasing chain length. Since the monomers are hooked together to form the chain, the coil must be a very loose object, possessing holes of all sizes. Considering now two chains with a large disparity of molecular weight, we can imagine that the compact small chain penetrates the holes of the large loose chain without experiencing much repulsion. At most it has to push away some strands of the large coil, which is easy since these strands are not stretched. This suggests that $a_2(y_1,y_2)$ should vanish if either y_1 and y_2 vanishes, which is guaranteed by our form but not by the form (3.9). Unfortunately, this argument is too qualitative to predict the analytic form of $a_2(y_1,y_2)$.

We believe that from these considerations it is plausible that the second virial coefficient decreases with increasing polydispersity, in contrast to Casassa's results. We note finally that eq 3.10 together with the numerical results given in Figure 6 suggests a very simple form of the polydispersity dependence of A_2. It follows that $a_2(y_1,y_2) \sim |a_2(y_1,y_1)a_2(y_2,y_2)|^{1/2}$ is a good approximation except for extreme values of y_1/y_2. Thus the form

$$A_2[p(y)] \simeq \left[\int_0^\infty dy\, p(y) y^{3/2\nu}\right]^2$$

should be a good approximation, except for very large polydispersity.

4. Concluding Remarks

In this work we have demonstrated the applicability of renormalization group calculations to osmotic pressure data. The calculation gives a reasonable fit to experiment up to concentrations where Flory–Huggins type mean field theories should apply. Clearly, more accurate data will reveal small systematic discrepancies between our calculation and experiment, which then will call for more accurate—and much more complicated—calculations. However, at the present level of accuracy we find full agreement between theory and experiment.

Our work on the polydispersity dependence of the osmotic pressure remains incomplete due to the lack of reliable data and the lack of a theory of the second virial coefficient in the limit of extreme disparity of chain length. Our work has stressed that virial coefficients cannot be extracted from experiment to a reasonable degree of accuracy without use of a theory valid at intermediate overlap. Indeed, the regime in which the osmotic pressure adequately is described in terms of its true low-order virial coefficients is very small. The virial coefficients usually extracted from experiment are effective quantities rather than true virial coefficients. Our theory holds for all overlap and therefore allows for a determination of true virial coefficients also from data taken at larger overlap.

We view this work as a first step in drawing a semiquantitative picture of the behavior of dilute polymer solutions. The directions in which this work should be extended are obvious. On the one hand, we should include the scaling variable z, thus connecting our results to those found near the Θ point. On the other hand, we should carry through a similar discussion of the scattering form factors. Work on the latter problem is in progress. In some respect our work comes 10 years late since meanwhile the interest has shifted away from dilute-solution properties. Nevertheless, we hope that it will stimulate accurate measurements, especially to get reliable information on the polydispersity dependence.

Acknowledgment. I am indebted to Professor T. A. Witten for many valuable discussions and a careful reading

of the manuscript. I thank Professor M. Gordon for bringing to my attention a number of useful references, and I am very much indebted to Professor I. Noda for sending me the original data underlying ref 28. A part of these data has been used in the analysis in connection with Figure 8.

References and Notes

(1) de Gennes, P. G. *Phys. Lett. A* **1972**, *38*, 339.
(2) des Cloizeaux, J. *J. Phys. (Orsay, Fr.)* **1975**, *36*, 281.
(3) de Gennes, P. G. *J. Phys., Lett. (Orsay, Fr.)* **1975**, *36*, L55.
(4) Schäfer, L.; Witten, T. A. *J. Phys. (Orsay, Fr.)* **1980**, *41*, 459.
(5) des Cloizeaux, J. *J. Phys. (Orsay, Fr.)* **1980**, *41*, 223. Schäfer, L.; Witten, T. A. *J. Chem. Phys.* **1977**, *66*, 2121.
(6) Yamakawa, H. "Modern Theory of Polymer Solutions"; Harper and Row: New York, 1971.
(7) Le Guillou, J. C.; Zinn-Justin, J. *Phys. Rev. Lett.* **1977**, *39*, 95.
(8) Knoll, A.; Schäfer, L.; Witten, T. A. *J. Phys. (Orsay, Fr.)* **1981**, *42*, 767.
(9) Krigbaum, W. R.; Flory, P. J. *J. Am. Chem. Soc.* **1953**, *75*, 1775.
(10) Casassa, E. F.; Stockmayer, W. H. *Polymer* **1962**, *3*, 53.
(11) Fox, T. G.; Kinsinger, J. B.; Mason, H. F.; Schuele, E. M. *Polymer* **1962**, *3*, 71.
(12) Kuwahara, N.; Oikawa, T.; Kaneko, M. *J. Chem. Phys.* **1968**, *49*, 4972.
(13) Kuwakara, N.; Okazawa, T.; Kaneko, M. *J. Polym. Sci., Part C* **1968**, *23*, 543.
(14) Kuwahara, N.; Okazawa, T.; Kaneko, M. *J. Chem. Phys.* **1967**, *47*, 3357.
(15) Schick, M. J.; Doty, P.; Zimm, B. H. *J. Am. Chem. Soc.* **1950**, *72*, 530.
(16) Schäfer, L.; Horner, H. *Z. Phys. B* **1978**, *29*, 251.
(17) Candau, F.; Strazielle, C.; Benoit, H. *Eur. Polym. J.* **1976**, *12*, 95.
(18) Stockmayer, W. H.; Casassa, E. F. *J. Chem. Phys.* **1952**, *20*, 1560.
(19) Sugamiya, K.; Kuwahara, N.; Kaneko, M. *Macromolecules* **1974**, *7*, 66.
(20) Flory, P. J.; Daoust, H. *J. Polym. Sci.* **1957**, *25*, 429. Leonard, J.; Daoust, H. *J. Phys. Chem.* **1965**, *69*, 1174.
(21) Fixman, M. *J. Chem. Phys.* **1960**, *33*, 370. *J. Polym. Sci.* **1960**, *47*, 91.
(22) Schulz, G. V.; Baumann, H.; Darskus, R. *J. Phys. Chem.* **1966**, *70*, 3647.
(23) Witten, T. A.; Schäfer, L. *J. Phys. A* **1978** *11*, 1843.
(24) Casassa, E. F. *Polymer* **1962**, *3*, 625.
(25) Kato, T.; Miyaso, K.; Nagasawa, M. *J. Phys. Chem.* **1968**, *72*, 2161.
(26) Chien, J. Y.; Shih, L. H.; Yu, S. C. *J. Polym. Sci.* **1958**, *29*, 117.
(27) Casassa, E. F. *Polymer* **1960**, *1*, 169.
(28) Noda, I.; Kitano, T.; Nagasawa, M. *J. Polym. Sci., Polym. Phys. Ed.* **1977**, *15*, 1129.
(29) Noda, I.; Kato, N.; Kitano, T.; Nagasawa, M. *Macromolecules* **1981**, *14*, 668.
(30) Suzuki, H. *Br. Polym. J.* **1977**, *9*, 222.
(31) Welzen, T. L. *Br. Polym. J.* **1980**, *12*, 95.
(32) Wallace, T. P.; Casassa, E. F. *Polym. Prepr., Am. Chem. Soc., Div. Polym. Chem.* **1970**, *11*, 136.
(33) Varadaiah, V. V.; Rao, V. S. *J. Polym. Sci.* **1961**, *50*, 31.
(34) Kato, T.; Miyaso, K.; Noda, I.; Fujimoto, T.; Nagasawa, M. *Macromolecules* **1970**, *3*, 777.

Computer Experiments on Branched-Chain Molecules

Kanji Kajiwara† and Walther Burchard*

Institut für makromolekulare Chemie der Universität, D-7800 Freiburg i.Br., West Germany. *Received July 21, 1981*

ABSTRACT: Star-shaped chain molecules with 4, 6, and 8 branches were simulated on a 5-choice simple cubic lattice according to Metropolis' scheme where the nearest-neighbor interactions were taken into account. Approximately 100 000 samplings were made for each chain over the Φ range 0.275–0.750. Here Φ denotes $-\epsilon/k_BT$, with ϵ being the attractive energy between a pair of unbonded units on the adjacent lattice sites; $\Phi_\Theta = 0.275$ corresponds to the Θ point as estimated by McCrackin et al. The data scattered considerably owing to branch segregation observed below the Θ point, so it was not possible to estimate the Θ point exactly. Taking $\Phi_\Theta = 0.275$ for branched chains as well, chain collapse was found to follow the equation based on the tricritical conjecture regardless of the number of branches.

1. Introduction

The Flory temperature (Θ point) is defined[1] as a reference point for chain configuration in solution in analogy with the Boyle temperature of an imperfect gas, where the binary interaction term vanishes. A linear chain is known to behave quasi-ideally[2] at the Θ point though the higher (ternary etc.) interaction terms have still nonzero values to spoil the exactness of the Θ point.[3] A quasi-ideal configuration of a linear chain is characterized by the proportionality of the second moment of chain distribution (the mean-square radius of gyration) to the chain length. However, its higher moments are not necessarily proportional to the corresponding powers of the chain length because of the nonzero values in the higher interaction terms, so the chain distribution is not strictly Gaussian. The most comprehensive view on the chain configuration just above the Θ point is offered by two-parameter theory,[4] which is based on Gaussian statistics and a δ-function binary interaction. The experimental data on linear-chain solutions are discussed satisfactorily in terms of two-parameter theory where the Θ point is estimated from the condition that the second virial coefficient is zero. In practice, the two-parameter approximation is satisfied for the linear-chain system. The two-parameter approximation fails when the attractive interaction becomes serious (below the Θ point) and chain molecules collapse to a rather dense form.[5]

As compared to a linear chain, a branched chain expands faster and its virial coefficient grows slower with increasing quality of solvent when the two-parameter approximation is applied to a branched-chain structure.[6] Though qualitatively correct, the two-parameter approximation fails in detail for the branched-chain system[8,9] probably because of the higher interaction terms due to increased segment density by branching. A depression of the Θ point was noted by branching[9-11] though this apparent depression may be caused again by the higher interaction terms (the third virial coefficient etc.).[12]

The characteristic changes of the conformational properties due to branching is often concealed by the mostly very pronounced heterogeneity with respect to size and structure. Classic examples are the osmotic pressure of

† On leave from the Institute for Chemical Research, Kyoto University, Uji, Kyoto-Fu 611, Japan.

0024-9297/82/2215-0660$01.25/0